

Los Alamos National Laboratory is operated by the University of California for the United States Department of Energy under contract W-7405-ENG-36

TITLE Gamma Ray Production Cross Section from Energetic Neutron
Inelastic Scattering for Methodical Improvements
in Planetary Gamma-Ray Spectroscopy

AUTHOR(S) C.M. Castaneda, R. Gearhart, & B. Sanii, Univ. Calif., Davis;
P.A.J. Englert, San Jose State Univ.; and
D.M. Drake and R.C. Reedy, SST-8

SUBMITTED TO Proceedings of Methods and Applications of Radioanalytical
Chemistry II, held in Kona, Hawaii on 21-27 April 1991.

DISCLAIMER

This report was prepared as an account of work sponsored by an agency of the United States Government. Neither the United States Government nor any agency thereof, nor any of their employees, makes any warranty, express or implied, or assumes any legal liability or responsibility for the accuracy, completeness, or usefulness of any information, apparatus, product, or process disclosed, or represents that its use would not infringe privately owned rights. Reference herein to any specific commercial product, process, or service by trade name, trademark, manufacturer, or otherwise does not necessarily constitute or imply its endorsement, recommendation, or favoring by the United States Government or any agency thereof. The views and opinions of authors expressed herein do not necessarily state or reflect those of the United States Government or any agency thereof.

By acceptance of this article, the publisher recognizes that the U.S. Government retains a nonexclusive, royalty-free license to publish or reproduce the published form of this contribution, or to allow others to do so, for U.S. Government purposes.

The Los Alamos National Laboratory requests that the publisher identify this article as work performed under the auspices of the U.S. Department of Energy.

Los Alamos Los Alamos National Laboratory
Los Alamos, New Mexico 87545

**GAMMA RAY PRODUCTION CROSS SECTION FROM
ENERGETIC NEUTRON INELASTIC SCATTERING
FOR METHODOICAL IMPROVEMENTS IN PLANETARY
GAMMA-RAY SPECTROSCOPY**

C.M. Castaneda, R. Gearhart, and B. Sani, Crocker Nuclear Laboratory, University of California, Davis, CA 95616, P.A.J. Englert, San Jose State University, San Jose, CA 95192, D.M. Drake and R.C. Reedy, Los Alamos National Laboratory, Los Alamos, NM 87545.

Abstract

Planetary Gamma ray spectroscopy can be used to chemically analyze the top soil from planets in future planetary missions. The production from inelastic neutron interaction plays an effective role in the determination on the C and H at the surface. The gamma ray production cross section from the strongest lines excited in the neutron bombardment of Fe have been measured by the use of a time analyzed quasi-mono-energetic neutron beam and a high purity germanium detector. The results from $E_n=6.5, 32, 43$, and 65 MeV are presented.

Introduction

One way to obtain information on the chemical composition of planetary surfaces such as those of the moon¹, asteroids and planets involves the measurement of energetic gamma-rays emitted from their surfaces. Only a few lines observable with a satellite based gamma-ray spectrometer come from naturally radioactive elements K, Th, and U. The majority of the lines are induced by the interaction of galactic cosmic rays (GCR) with the planetary surface and can be related to the induced nuclear reaction and the target element². The GCR consists mainly of energetic charged particles, of which about 90% are protons and 10% alpha particles³. In the case of the protons, the maximum of the differential flux lies at about 600 MeV, whereas the mean energy is about 2-3 GeV. When such energetic particles hit solid matter, a cascade of secondary hadrons develops. Of these cascades those that produce neutrons are especially important for the production of gamma-rays. Nonelastic scattering and neutron capture reactions produce many characteristic gamma-ray lines of discrete energy. A few lines are also produced from proton and neutron spallation induced reactions, and a very small number from the decay of radioactive nuclei built up by all of these nuclear reactions. The similarity in principle to prompt gamma activation analytical techniques is evident. The

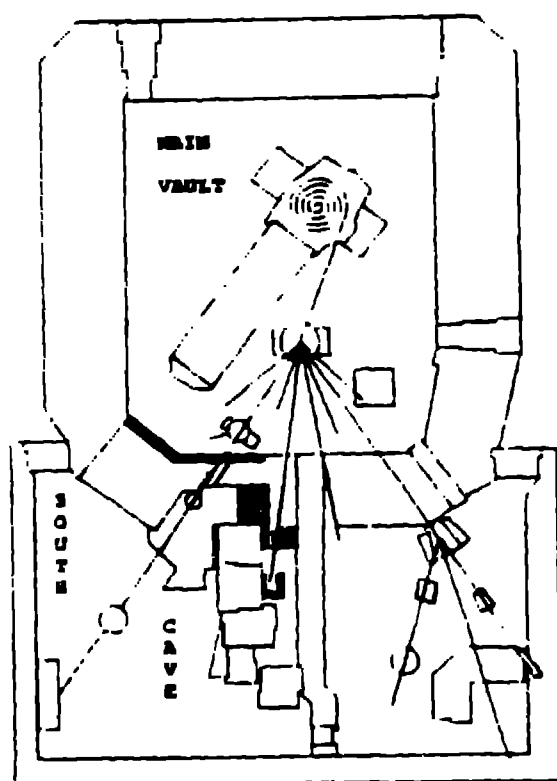


Fig. 1a.

Fig. 1b.

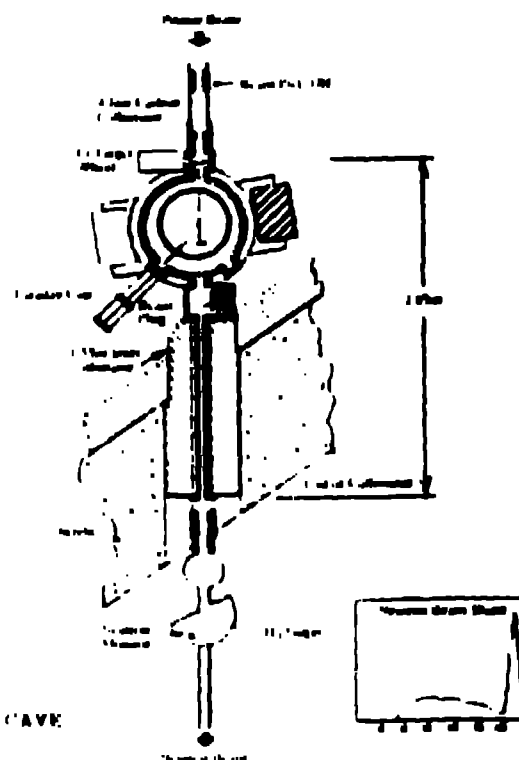


Fig. 1a. Beam lay out of the Oak Ridge Nuclear Laboratory Cyclotron.
 Fig. 1b. Neutron production facility and neutron monitor system.
 The gamma-ray production target is further to the right. The
 neutron beam is transported into vacuum to the gamma-ray
 production chamber.

major difference, however, to terrestrial applications of prompt activation methods 4,5 that complicates the analysis or data reduction is that a direct comparison to standards is not possible. No such ground standards will be available, as no mission returning samples from planets or smaller planets are planned in the near future. However, semi-empirical models of energy spectra and fluxes of reacting secondary hadrons are available that enable a rough estimate of expected gamma-ray fluxes. While neutron capture cross-sections are reasonably well known, cross-sections for inelastic scattering reactions leading to analytical useful gamma radiation are practically not known for major rock-forming elements. For a straight forward data analysis of gamma-ray spectra from a planetary surface, neutron induced gamma-ray cross-sections have to be measured for neutron energies between 0.5 and 150 MeV for a variety of soil component elements. In our experiments we have used a quasi-monoenergetic neutron beam at energies of 6.5, 32, 43 and 65 MeV to bombard major planet-forming elements to measure the production cross section for their gamma-rays signature. This and further research will allow gamma-ray spectroscopy to be used to measure relative and absolute abundances of elements in a planetary surface.

Experimental Method

The experiments were performed using the unpolarized neutron beam facility of the Crocker Nuclear Laboratory (CNL) at University of California Davis⁶. The nearly monoenergetic neutron beam was produced via the ${}^7\text{Li}(p,n){}^6\text{Be}$ reaction and limiting the neutrons to those emitted at zero degrees. Fig. 1a shows the floor plan of CNL with the beam layout of the cyclotron. The neutron source is located inside the main vault and the neutrons associated with the accelerator are confined to the vault area; the wall between the experimental area and the cyclotron room is formed from 30.5 cm of steel and 1.2 m of ordinary concrete that gives an attenuation of ≈ 103 for 65 MeV neutrons. Fig. 1b shows the main features of the neutron production system⁷. The proton beam is steered and focused on a lithium target and subsequently swept by a clearing magnet to the Faraday cup. The neutrons are produced by the reaction ${}^7\text{Li}(p,n){}^6\text{Be}$ and collimated to 0° and the beam size defined to 0.03 msr. Fig. 2a. Neutron energy spectrum. Between 50-60% of all the neutrons come from the ${}^7\text{Li}(p,n)$ ground state transition at 0° . Fig. 2b. Time spectrum from the neutron beam from the HPGe detector. The prompt time cut encloses the peak and is 13ns wide. The random cut is equally wide and to the left of the prompt peak.

A proton recoil telescope is used to monitor the beam. The telescope is made of an E-IE detector 20 cm from a thin (${}^6\text{Li}$ target (4.17 mg/cm²) located 503 cm downstream of the neutron production target. Events produced by the n-p reaction in the ${}^6\text{Li}$ target are particle and time analyzed and stored event by event to get a neutron beam energy profile, Fig. 3a. This is accomplished by using the Rindback parameterization of the n-p differential.

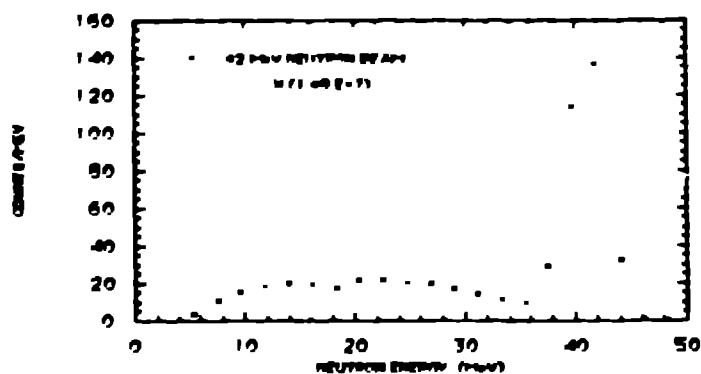


Fig. 2a.

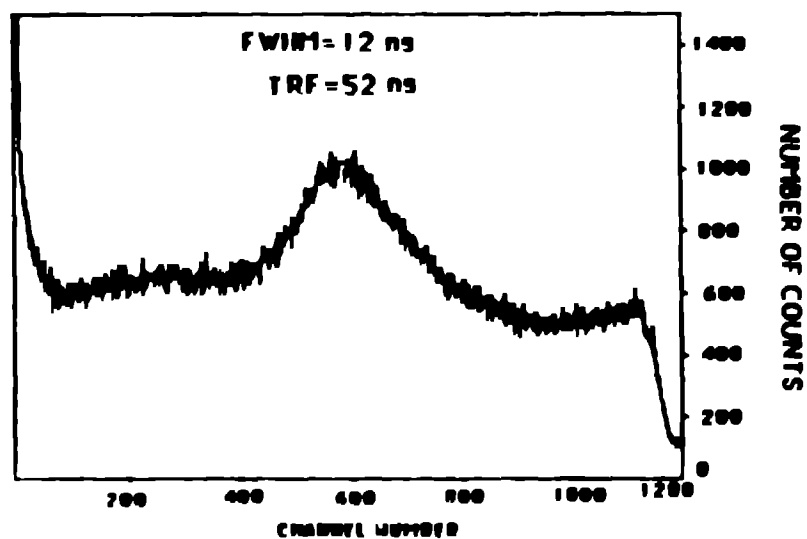


Fig. 2b.

Fig. 2a. Neutron energy spectrum. Between 50-60% of all the neutrons come from the ${}^7\text{Li}(p,n)$ ground state transition at 0 $^\circ$.

Fig. 2b. Time spectrum from the neutron beam from the HPGe detector. The prompt time cut encloses the peak and is 13ns wide. The random cut is equally wide and to the left of the prompt peak.

cross section. The absolute normalization is obtained through the use of that energy profile and is double checked by integrating the proton beam impinging on the ${}^7\text{Li}$ target and using the 0° differential cross section for the ${}^7\text{Li}(p,n){}^7\text{Be}^0$. The irradiated targets were 927 cm from the neutron production target and the cyclotron vacuum extended to 38 cm from the gamma production target, the rest of the beam pipe was filled with circulating helium gas to minimize background from the air in the cave. The gamma spectrum was detected in a High Purity Germanium spectrometer and recorded event by event with time and energy parameters saved for later analysis. The detector was placed 40 cm from the gamma target and 135 degrees from the neutron beam line. The detector was in a lead tube lined with copper and cadmium sheets. The neutron beam dump was 203 cm from the target and was 28 cm of water thick and surrounded by a combination of iron, lead and concrete 7.5 cm, 5cm and 75 cm thick respectively. We time analyzed the gamma-ray spectrum to get a prompt section and a random section which we subtracted from the prompt spectrum to obtain the gamma rays that were only produced by the high energy neutron peak. Fig. 2b shows the time spectrum from the HPGe detector for 43 MeV neutrons. The intrinsic time resolution of the HPGe spectrometer was determined to be around 12ns by using a ${}^{60}\text{Co}$ source and a NaI(Tl) detector in coincidence with the HPGe detector. The energy resolution for the gamma detector was 1.8 Kev at 1332 KeV and no deterioration was noticed at the end of the experiment. The efficiency of the detector was determined with a NIST source using the experiment's geometry; corrections for gamma attenuation and dead times were applied to the cross section calculations.

Gamma spectrum were obtained for natural Mg, Al, Si, Fe, S, CaCO_3 , Si, SiO_2 , Mg and C targets ranging in thickness from 1.3 to 8 g/cm². The neutron energies used were 65 ± 0.9 , 43 ± 1.2 and 32 ± 1.6 MeV, and for Fe and Al at 6.5 ± 2.0 MeV. In this paper we will only discuss the Fe target results. Runs were made to evaluate the room background when the beam was in the cave and no target was being irradiated. Also, the contributions from the Faraday cup and the main vault leakage were measured by placing the neutron production target wheel empty slot.

Results and Discussions

Fig. 3a. shows the raw data for the gamma ray spectrum from the $\text{Fe}(n,\gamma)$ reaction. The observed prominent peaks come from the (n,γ) , $(n,2n\gamma)$, $(n,pn\gamma)$, and $(n,n\alpha\gamma)$ channels. Peaks from other sources are observed, especially those from the interaction of target emitted neutrons with the detector crystal. Fig. 3b shows the no target spectrum which clearly demonstrates the low background.

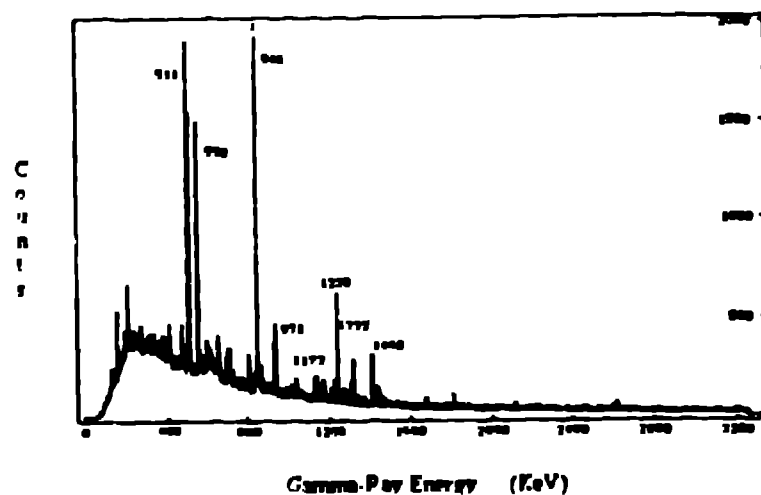


Fig. 3a.

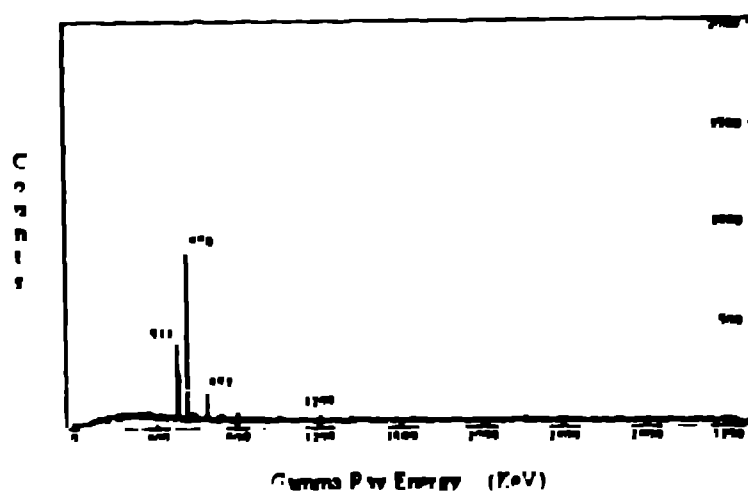


Fig. 3b.

Fig. 3a. Gamma-ray spectrum from $\text{Fe}(n,xy)$ reaction for 43 MeV neutrons. The inelastic peaks in germanium from the $\text{Ge}(n,n')$ reaction are produced by neutrons coming from the Fe target.

Fig. 3b. Gamma-ray spectrum for an empty target. This background comes from the interaction of the primary protons with the Faraday cup in the cyclotron room and from the interaction of the neutron beam with the beam dump.

produced by the neutron beam with the cave surroundings and that the Ge lines are produced by neutrons emitted by the target. The Ge lines are prominent in both the random and prompt contributions for the Fe target and cancel out. By comparing the spectrum from the high energy peak (prompt) with the spectrum generated by the tail (random) we see in both, the same lines with almost the same intensity. This makes it essential to use a time-of-flight technique to sort the energy dependence of the gamma-ray production. The situation is further complicated by the fact that the tendency is for the cross section to go up when the neutron energy goes down. By using quasi-monoenergetic neutrons, we compensate the difference in cross section by enhancing the high energy neutrons and decreasing the yield at the lower energies.

TABLE 1

Gamma-ray production cross section from a thin iron target bombarded by a quasi-monoenergetic neutron beam of energy 6.5, 32, 43 and 65 MeV. The cross sections were obtained by time analysing the neutron beam and using only the contribution from the high energy peak of the neutron energy spectrum.

ENERGY (KeV)	REACTION	CROSS SECTION (mb)			
		65.MeV	43.MeV	32.MeV	6.5MeV
511.0	e ⁺ Annih.	304.2	248.	332.	
558.0		79.4	84.9	35.3	
803.5	²⁰⁸ Pb (n, nγ)	18.5	12.7	35.3	
846.8	⁵⁶ Fe (n, nγ)	299.4	303.7	531.4	1800.0
858.2	⁵⁶ Fe (n, npγ)		17.4	24.3	
931.3	⁵⁶ Fe (n, 2nγ)	49.4	73.4	77.8	
935.5	⁵⁶ Fe (n, nαγ)	22.4		17.9	
1027.9	⁵⁶ Fe (n, nγ)		37.5	19.3	
1130.2	²⁷ Al (n, npγ)		38.0	75.3	
1166.2	⁵⁶ Fe (n, npγ)		37.0	31.3	
1173.6	⁶⁰ Co decay		4.2	22.8	
1222.7		9.6	31.4	38.9	
1228.5	⁵⁶ Fe (n, nγ)	65.1	55.1	98.3	372.0
1303.5			21.5	13.5	
1316.5	⁵⁶ Fe (n, 2nγ)	37.4	18.7	56.5	
1333.1	⁵⁶ Fe (n, nαγ)	17.5	9.6	31.8	
1408.4	⁵⁶ Fe (n, nγ)	43.4	148.7	157.2	
1424.7	⁵⁶ Fe (n, nαγ)	66.7	10.0	61.7	
1810.7	⁵⁶ Fe (n, nγ)	73.4	47.7	19.2	122.0
2112.5	⁵⁶ Fe (n, nγ)		20.4	13.3	

Table 1 summarizes the cross section for gamma-rays produced from iron. In general, these cross sections decrease as the neutron energy goes up or they look fairly constant in the energy interval we measured. The error bars in this experiment vary from 10 to 15%, depending on the statistics of the intensities for the peaks in the prompt and random spectra. Fig. 4, shows the data from Oak Ridge³ for the 846 KeV and the 931 KeV peaks from the iron target from threshold to 40 MeV as compared with this experiment. The present experiment gives values that are higher than those that one would extrapolate from Ref. 9. These discrepancies are not yet understood and are difficult to understand in light of the agreement we observe for the ^{55}Fe transition at 931 KeV. Although, in this energy region Ref. 9 reports interference with the Linac gamma-flash which could have increased the 931 KeV yields. The low energy point at 6.5 MeV shows very good agreement for the ^{56}Fe transition at 847 KeV. One could argue that they included the carbon contribution in the absolute measurement of the flux by which they increased the neutron flux and therefore lower the gamma-ray yields.

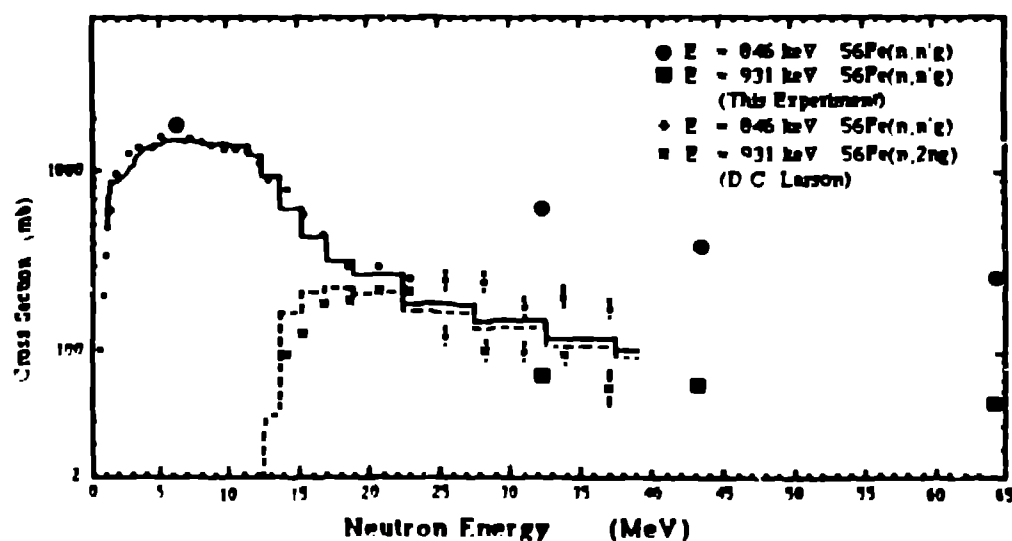


Fig. 4.

Fig. 4. Excitation function for the 846 KeV and the 931 KeV peaks. Results from Oakridge are shown to compare with present results.

Conclusions

To remotely analyze the surface of the planets by means of nuclear techniques one needs to know the gamma ray production cross sections from neutron capture as well as for their inelastic interaction with the soil elements. The ratio between the yields from these two processes ($(n,\gamma)/(n,n\gamma)$) will also give information on the amount of moderating materials (H,C) present in the surface. Although the capture cross sections are very well established the neutron inelastic cross sections are not so firm. To reliably use the ratio of the gamma ray production by inelastic neutron scattering to the one from the neutron capture as a sound radioanalytical tool, one has to measure the inelastic production cross section with a time analyzed beam which will differentiate the contributions from different parts of the neutron beam.

ACKNOWLEDGEMENT

We would like to thank Joel McCurdy and the CNL Cyclotron crew in delivering the beam for these experiments. Many thanks to Walter Kemmler and his mechanical shop staff for providing help in the beam alignment and vacuum technical support. We also thank Dr. John Young for his help in the runs and undergraduate students Dan McLaughlin, Warna Hettiarachchi and Doug Gearhart for carrying the attenuation measurements for the targets.

References

1. J.R. ARNOLD, A.E. METZGER, R.C. REEDY. Proc. 8th Lunar Science Conf., 1977, p.945.
2. R.C. REEDY, Proc. 9th Lunar Science Conf., 1978, p. 2961.
3. M. GARCIA-MUNOS, J.A. SIMPSON, Proc. 16th Int.Conf. on Cosmic Rays, OG-6-3, 1979, p.270.
4. L.G. EVANS. J.I. TROMBA, J.R. LAPIDES, D.H. JENSEN, IEEE, Trans. Nucl. Sci., NS28 (1980) 1226.
5. M.R. WORMLAND, C.G. CLAYTON, Journal Appl. Radiation Isotopes, 34 (1983) 71.
6. J.A. JUNGGERMAN, F.P. BRADY, NIM, 89 (1970) 167-172.
7. J. BINSTOCK, Phys. Rev., C10 (1974) p.19.
8. J.R. ROMERO, F.P. BRADY, J.A. JUNGGERMAN, NIM, 134 (1976) 537-539.
9. D.C. LARSON, Radiation Effects, 1986, Vol. 92 I 4, pp. 71-82.